Mg^{2+} Binding to Alkaline Phosphatase Correlates with Slow Changes in Protein Lability†

Eric Dirnbach,[‡,§] Duncan G. Steel,[§,||,⊥] and Ari Gafni*[,§,#]

Biophysics Research Division, Departments of Biological Chemistry, Electrical Engineering and Computer Science, and Physics, and Institute of Gerontology, University of Michigan, Ann Arbor, Michigan 48109

Received July 5, 2001

ABSTRACT: The in vitro reactivation of unfolded *Escherichia coli* alkaline phosphatase (AP) in the presence of the two natively bound metals Zn^{2+} and Mg^{2+} produces two protein species, characterized by different guanidine hydrochloride denaturation kinetics. The high-lability AP form slowly converts to the low-lability form in a first-order reaction with a characteristic lifetime (inverse rate constant) of approximately 300 h at pH 8.0 and 25 °C. Addition of Zn^{2+} and Mg^{2+} ligands to (folded) apo-AP also produces two protein species, with denaturation kinetics and a long conversion lifetime similar to those found in refolding AP. In contrast, adding Zn^{2+} alone to apo-AP produces only the high-lability species with no subsequent structural change, suggesting that Mg^{2+} binding is the event which is responsible for the production of the low-lability AP. The rate of conversion from high- to low-lability AP was found to be linearly dependent on Mg^{2+} concentration, indicating that Mg^{2+} binding is rate limiting for this reaction. Experiments where either Zn^{2+} or Mg^{2+} was added first, with the second metal added later, show that Mg^{2+} binding is slowed by the prior presence of bound Zn^{2+}. Mg^{2+} binding to Zn-AP also slightly increases the enzymatic activity; however, the extent of formation of the low-lability species is related to the square of the Mg^{2+}-induced activity increase. Thus the binding of two Mg^{2+} to AP produces the dramatic reduction in the rate of denaturation that characterizes the low-lability species. The data suggest the possibility of long distance intersubunit interactions and a role for Mg^{2+} in providing "kinetic stability" for AP.

The protein folding process is generally believed to result in a unique, thermodynamically stable conformation that is fully determined by the amino acid sequence (*1*). Many small, single-domain, proteins can be adequately modeled as simple two-state systems, with only the denatured and native states significantly populated (*2*, *3*). For most proteins, however, the native state is attained through a much more complex process. Some proteins have well-populated intermediate species, and their slow folding is caused by proline isomerization or disulfide bond rearrangement (*4*−*6*). For larger, multidomain or multisubunit proteins, slow domain rearrangements or oligomerization results in a more complicated pathway toward the native state (*7*, *8*). Moreover, for proteins with bound ligands that are essential for enzymatic activity and/or thermodynamic stability, the attainment of the native state must also involve the incorporation of these ligands (*8*). As discussed in this paper, ligand binding may be a surprisingly slow event, with important ramifications for the development of the structurally mature protein.

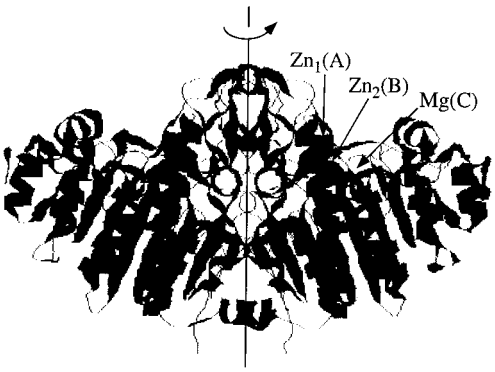

FIGURE 1: Ribbon diagram of the AP structure with two Zn^{2+} and one Mg^{2+} binding sites indicated at the monomer active site (*11*). The A−B−C metal site notation is also shown. The two monomers are shaded differently, and the 2-fold axis of monomer rotation is indicated. The central 10-strand β-sheet, flanked by α-helices, spans each monomer structure.

The current work involves AP,[1] a 94 kDa homodimeric periplasmic enzyme with 449 amino acid residues per monomer (*10*), that binds two Zn^{2+} and one Mg^{2+} per active site (*11*). Zn^{2+} binding to this nonspecific phosphomonoesterase is required for both catalysis and thermodynamic stability. Mg^{2+} is not essential but enhances both characteristics (*12*, *13*). Figure 1 shows the AP dimer structure with metal binding sites indicated. These sites have been desig-

† This work was supported by National Institutes of Health Grants AG09761, 5T32GM08270-06, and T32AG00114.

* To whom correspondence should be addressed at the Institute of Gerontology, Room 913, 300 North Ingalls St., University of Michigan, Ann Arbor, MI 48109. Phone: (734) 936-2156. Fax: (734) 936-2116. E-mail: arigafni@umich.edu.

‡ Biophysics Research Division.

§ Institute of Gerontology.

|| Department of Electrical Engineering and Computer Science.

⊥ Department of Physics.

Department of Biological Chemistry.

[1] Abbreviations: AP, alkaline phosphatase; GdnHCl, guanidine hydrochloride; p-NPP, *p*-nitrophenyl phosphate; EPPS, *N*-(2-hydroxyethyl)piperazine-*N*′-3-propanesulfonic acid; CD, circular dichroism.

10.1021/bi011399m CCC: $20.00
Published on Web 08/18/2001

nated A, B, and C in NMR studies, according to decreasing order of metal binding affinity (*14*−*16*). The A and B sites are the two classes of Zn^{2+} binding sites, with the A sites binding the first Zn^{2+} pair and the B sites binding the second pair. The B sites bind Zn^{2+} more strongly in the presence of phosphate and can also bind Mg^{2+} at high concentrations (*14*); however, Mg^{2+} normally occupies the C sites. There appears to be significant cooperativity among metal binding sites and between the two subunits (*15*, *17*−*21*).

During its in vitro renaturation from the GdnHCl denatured state, *Escherichia coli* alkaline phosphatase (AP)[1] displays slow conformational changes on an unusually long time scale compared with the recovery of the majority of enzymatic activity. This process has been shown to involve a conversion between two discrete species with very different susceptibilities to GdnHCl denaturation (*9*). The long lifetime of this structural change complicates the conventional notion that the "native" state and "enzymatically active" state are necessarily identical.

Previous investigations in this laboratory have examined the possible role of proline isomerization in the observed slow structural changes in AP during refolding, a mechanism that has been implicated in slow-folding events in other proteins (*22*−*25*). No evidence supporting proline isomerization as a rate-limiting folding step for AP was found (*26*). In the present paper, we focus on the role of the metal ligands, and in particular Mg^{2+}, as the cause of these slow events. The binding of metal ions to metal-depleted, apo, AP was followed, and data to support a role for Mg^{2+} binding in the observed lability changes are presented. There is also evidence for substantial structural changes caused by the binding of two Mg^{2+}, possibly involving long distance intersubunit interactions.

EXPERIMENTAL PROCEDURES

Enzymes and Reagents. All AP used in these experiments was expressed in the *E. coli* strain SM547 using the plasmid pEK154. The cells with overexpressed AP were osmotically shocked to release periplasmic proteins, which include AP. AP purification was performed as described elsewhere (*27*) with an ammonium sulfate precipitation, followed by dialysis in TMZP buffer (10 mM Tris, 1 mM $MgCl_2$, 10 μM $ZnSO_4$, 100 μM NaH_2PO_4, 5 mM NaN_3, pH 7.4) and ion-exchange chromatography. The purified AP was determined by SDS−PAGE to be greater than 95% homogeneous.

Preparation of Apo-AP Stock Solution. The AP used in these experiments was first rendered metal free (apo) by an ammonium sulfate dialysis procedure (*15*), where AP was dialyzed twice against 2 M $(NH_4)_2SO_4$, pH 9.0, followed by exchange into metal-free 10 mM Tris, pH 9.0, and then into 100 mM Tris, pH 8.0, with a Centricon 30. A number of Centricon spins were performed to ensure that the final ammonium sulfate concentration was subnanomolar. The apo-AP stock solution was concentrated to at least 60 mg/mL and stored at 4 °C until use. AP concentrations were determined spectrophotometrically at 278 nm using $A_{278}^{0.1\%} = 0.72$ (*28*). The final activity of apo-AP was typically less than 4% of holo-AP.

Preparation of Metal-Free Buffers and Cuvettes. All buffers were made metal free by passing them through an equilibrated Chelex 100 column. All quartz and plastic cuvettes were made metal free by washing extensively with HCl or nitric acid, followed by a thorough rinsing with metal-free water.

Denaturation and Refolding of AP. AP at 10 mg/mL was denatured in 6 M GdnHCl and 100 mM Tris, pH 8.0. Refolding was accomplished by a 100-fold dilution into 100 mM Tris, pH 8.0, with 0.1 mM $ZnCl_2$ and 0.1 mM $MgCl_2$ added. The final AP concentration was 0.1 mg/mL.

AP Activity Assay. AP activity was followed with the standard spectrophotometric assay (*29*). A 10 μL AP sample was added to 0.9 mL of the AP assay mixture (1 M Tris, 1 mM p-NPP) in a 1 cm path-length cuvette. The change in absorbance due to the hydrolysis of p-NPP at 25 °C was monitored for 30 s at 410 nm (Milton Roy spectrophotometer).

Circular Dichroism Spectra. The circular dichroism (CD) spectra of 0.5 mg/mL AP in 10 mM EPPS and 100 mM NaCl, pH 7.5, buffer under various metal conditions were measured at 25 °C. All CD experiments were conducted with a 2 mm path-length quartz cuvette using a Jasco J-715 spectropolarimeter.

Thermal Unfolding Curves. The CD signal at 222 nm was monitored to assess the extent of unfolding of 0.5 mg/mL AP in 10 mM EPPS and 100 mM NaCl, pH 7.5 buffer, under various metal conditions during a temperature ramp from 25 to 100 °C. The data were converted to the fraction of folded protein by normalizing to the maximum and minimum CD signal on the temperature range.

Lability Experiment. The lability of AP is a measure of the rate of its denaturation and is thus a kinetic parameter reflecting the activation energy of unfolding. Lability was measured by exposing enzyme samples to 4.5 M GdnHCl at 25 °C and pH 8.0 and monitoring the loss of AP activity as a function of time. The activity values were expressed as a percentage of the starting activity of the sample. Control lability was determined by using native metal-equilibrated AP that had not been unfolded and refolded.

Analysis of Lability Data. All denaturation curves were fit using a two-exponential decay. The set of curves (as a function of refolding time) for each AP sample, along with the control curves, was analyzed globally (Excel) using a least-squares analysis with two common unfolding time constants and allowing the preexponential terms to vary individually, with their sum set to 1. The rate of decrease of the amplitude of the highly labile fraction (smaller τ) over refolding time, normalized to the control (equilibrium) level, determines the rate of conformational change between the two AP lability states. This lability conversion was found to follow an exponential decay law, and the inverse of the observed rate of this process is the lifetime for the lability conversion. All lability decay times and conformational conversion lifetimes were calculated from the average of three samples.

Comparison of AP Activity and Lability. Activity and lability of AP at 0.1 mg/mL were determined under two conditions: (1) refolding AP in the presence of 0.1 mM $ZnCl_2$ and 0.1 mM $MgCl_2$ and assaying activity and lability over time; (2) adding increasing amounts of $MgCl_2$ (5 μM to 5 mM) to apo-AP, followed by 0.1 mM $ZnCl_2$, and assaying samples after equilibrium has been attained. The lability experiments for condition 2 were conducted using a

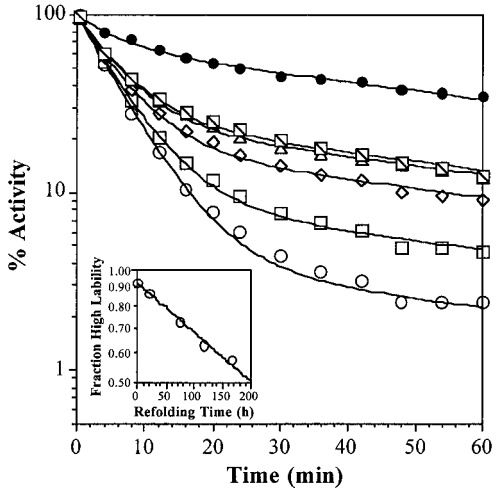

FIGURE 2: AP lability conversion as a function of refolding time. After complete denaturation, AP was refolded for various times with buffer containing 0.1 mM $ZnCl_2$ and 0.1 mM $MgCl_2$. Aliquots of the refolding enzyme solution were then taken at different times and subjected to a second denaturation with 4.5 M GdnHCl at 25 °C and pH 8.0. The individual curves depict activity as a function of incubation time in 4.5 M GdnHCl for AP at the following times after the initiation of refolding: ●, control (nondenatured native AP); ○, 2 h; □, 23 h; ◇, 74 h; △, 118 h; □ with backslash, 166 h. The activity is expressed as a percentage of starting activity of that sample before denaturation. All curves are fit globally to two exponentials with common lifetimes that averaged 6.3 ± 0.2 and 93.5 ± 6.5 min. Inset: The fraction of high-lability (fast decay) AP, normalized to the control level, is plotted over refolding time. The data were fit to a single exponential decay that represents the rate of conversion between high- and low-lability AP, with the inverse rate representing the conversion lifetime. The decrease in the fraction of high-lability AP occurred with a lifetime of 294 ± 17 h.

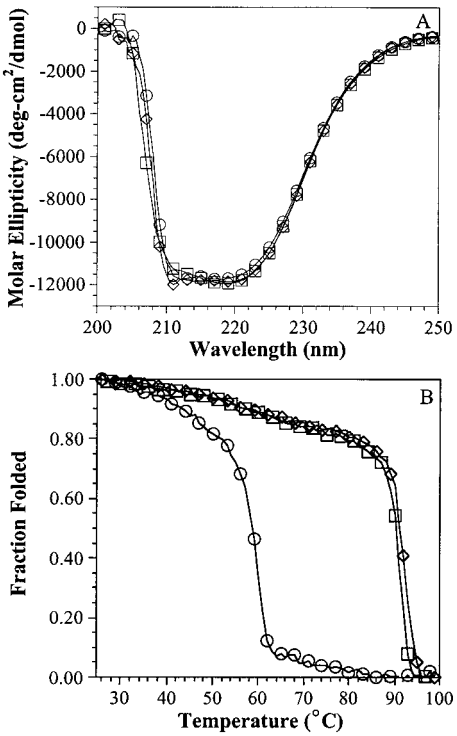

FIGURE 3: Comparison of metal-free (apo) and metal-bound (holo) AP. (A) CD spectra of 0.5 mg/mL AP in 10 mM EPPS and 100 mM NaCl, pH 7.5 buffer at 25 °C under the following conditions: ○, apo-AP; □, AP with 0.1 mM $ZnCl_2$; ◇, AP with 0.1 mM $ZnCl_2$ and 1.0 mM $MgCl_2$ (holo-AP). (B) CD (222 nm) monitored unfolding of 0.5 mg/mL AP in 10 mM EPPS and 100 mM NaCl, pH 7.5 buffer under the following conditions: ○, apo-AP; □, AP with 0.1 mM $ZnCl_2$; ◇, AP with 0.1 mM $ZnCl_2$ and 1.0 mM $MgCl_2$ (holo-AP). The unfolding midpoint of the apo-AP is 59 °C, Zn-AP is 91 °C, and holo-AP is 92 °C. For comparison purposes, the raw CD data were converted to the fraction of folded protein by normalizing to the maximum and minimum CD signal on the temperature range.

5 M GdnHCl denaturation for 30 min. The activity increase due to Mg^{2+} binding was expressed in both cases as a fraction between zero (Zn-AP) and the maximum activity at 5 mM $MgCl_2$. The fraction of low-lability AP was determined as described above.

Power-Law Fit of Activity−Lability Data. The AP activity−lability comparison data were compared to a model which assumed that each bound Mg^{2+} contributes equally to activity but that two bound Mg^{2+} are needed for the formation of the low-lability AP. Using this model, a calculation of activity and low-lability fractions under various Mg conditions results in a squared power-law relationship: fraction lability = (fraction activity)^2. This model is compared to the experiment by fitting the data to the power-law equation and determining the exponent.

RESULTS

AP that has been denatured in 6 M GdnHCl and then refolded attains nearly all of its original biological activity; however, the renatured enzyme displays biexponential GdnHCl denaturation kinetics. The two components seen in the denaturation represent two distinct species, referred to here as "high lability" and "low lability" (Figure 2). The high- and low-lability species have globally fit decay times of 6.3 ± 0.2 and 93.5 ± 6.5 min, respectively, under the conditions used. Over time, the fraction of AP that is more susceptible to denaturation (high lability) decreases as it is converted to the AP species that is less susceptible to denaturation (low lability). Under the experimental conditions used, 25 °C and pH 8.0, this process has a conversion lifetime of 294 ± 17 h.

To determine the role of metal binding in this behavior, a reactivation experiment was initiated using AP that has not been denatured, but with all metal ligands removed. This apo-AP is in a conformation that is nearly completely folded and dimerized, though, without the metal ligands, it is much less stable and completely inactive (*30*−*33*). As shown in Figure 3A, apo-AP has a CD spectrum nearly identical to that of Zn-AP or to holo-AP (both Zn^{2+} and Mg^{2+} bound), confirming its nearly intact secondary structure content. However, upon heating, apo-AP unfolds at a much lower temperature than Zn-AP or holo-AP (Figure 3B), reflecting in part the reduced stability in the absence of the metal ligands (*34*). The T_m values for Zn-AP and holo-AP differ slightly (91 and 92 °C, respectively), reflecting the small additional thermodynamic stability that results from Mg^{2+} binding, as compared with Zn^{2+} binding, which is responsible for the majority of the increased stability over apo-AP.

When excess Zn^{2+} and Mg^{2+} were added to apo-AP, and the protein's GdnHCl denaturation kinetics was subsequently monitored as before (Figure 4), high- and low-lability species were found, and as before, they displayed globally fit decay times of 6.6 ± 0.2 and 92.3 ± 4.9 min, respectively, which are nearly identical to those of freshly refolded holo-AP. A

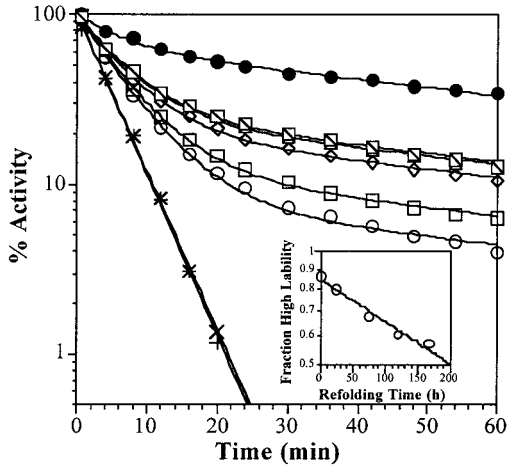

FIGURE 4: Lability of AP over time after metal addition. Lability curves for AP at the indicated times after the addition of 0.1 mM $ZnCl_2$ and 0.1 mM $MgCl_2$ to apo-AP: ●, control (holo-AP); ○, 2 h; □, 23 h; ◇, 74 h; △, 118 h; □ with backslash, 166 h. Lability curves after the addition of only 0.1 mM $ZnCl_2$ to apo-AP: ×, 2 h; +, 166 h. The activity is expressed as a percentage of starting activity of that sample before denaturation. All curves from samples with both Zn^{2+} and Mg^{2+} are fit globally to two exponentials with common decay times that averaged 6.6 ± 0.2 and 92.3 ± 4.9 min. The two curves for only $ZnCl_2$ are fit to a single exponential with decay times of 4.7 ± 0.1 and 4.6 ± 0.1 min, respectively. Inset: For the curves representing AP with both Zn^{2+} and Mg^{2+}, the fraction of high-lability (fast decay) AP is normalized to the control level and plotted over incubation time. The data were fit to a single exponential decay that represents the rate of conversion between high- and low-lability AP, with the inverse rate representing the conversion lifetime. The decrease in the fraction of high-lability AP occurred with a lifetime of 308 ± 24 h.

lifetime of 308 ± 24 h was found for the transition from the high-lability to the low-lability AP, again in good agreement with that of freshly refolded holo-AP. It thus appears that the addition of metals to folded apo-AP produces behavior very similar to that of AP refolded from the denatured state. In addition, apo-AP to which only Zn^{2+} has been added quickly regained 80−90% of the enzymatic activity of holo-AP but displayed GdnHCl denaturation kinetics that was similar (though not identical) to that of the high-lability state, with a decay time of 4.7 ± 0.1 min. Over time, this high-lability AP did not convert to low-lability AP, in contrast to what was observed when both metals were present.

It appears from these experiments that AP with only Zn^{2+} bound exists exclusively as the high-lability species and that it is the presence of Mg^{2+} that produces the low-lability AP. Three explanations that could account for this behavior were considered: (1) fast Mg^{2+} binding to Zn-AP triggers slow conformational changes leading to the production of low-lability AP; (2) the Zn-AP species itself undergoes a slow conformational change before it can bind Mg^{2+} and then quickly converts to low-lability AP; (3) Mg^{2+} binding to Zn-AP is the slow event, and this binding converts the AP to the low-lability species. Figure 5 shows these possible pathways in a simplified metal binding reaction scheme. To distinguish between these three possibilities, apo-AP was mixed with a constant concentration of Zn^{2+} and increasing concentrations of Mg^{2+} and assayed for lability over time. The rate of lability conversion was found to have a linear dependence on the concentration of Mg^{2+}, as shown in Figure 6. As only pathway 3 would show any Mg^{2+} concentration

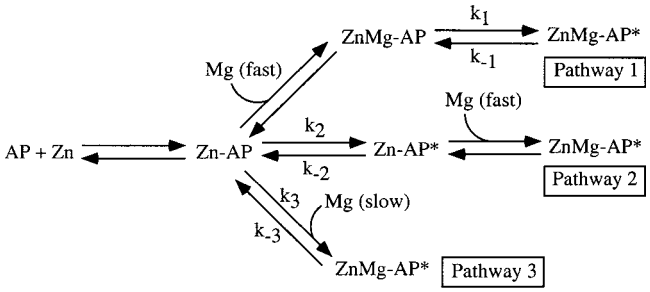

FIGURE 5: Possible pathways for an AP−Mg binding scheme. A simplified reaction scheme depicting three possible pathways for the formation of the low-lability AP state, through the binding of two Mg^{2+} to an AP dimer that already has fully bound Zn^{2+}. Only one Mg binding reaction is shown for simplicity. Pathway 1: fast Mg^{2+} binding followed by slow conformational change. Pathway 2: slow conformational change of the Zn-AP species followed by fast Mg^{2+} binding. Pathway 3: slow Mg^{2+} binding to Zn-AP leading to the low-lability AP state. Only the forward and reverse reaction rates (k) associated with the rate-limiting lability conversion step are shown. Zn-AP* represents a species that has undergone an internal conformational change, and ZnMg-AP* represents the low-lability AP state.

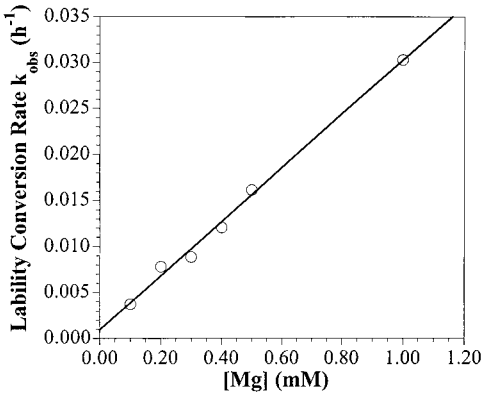

FIGURE 6: Lability conversion rate of AP vs Mg^{2+} concentration. The rate of conversion (k_{obs}) of the high-lability to low-lability AP is plotted for various Mg^{2+} concentrations. Assuming pathway 3 from Figure 5, the reversible binding reaction rate $k_{obs} = k_{-3} + k_3[Mg]$. The linear fit gives rate $k_3 = 29.3 \pm 1.1\ M^{-1}\ h^{-1}$, and the reverse rate $k_{-3} = (9.2 \pm 5.6) \times 10^{-4}\ h^{-1}$.

dependence of the slow step, this result supports the "slow Mg^{2+} binding" hypothesis. From the slope and intercept of the lability conversion rate curve, we determine that $k_3 = 29.3 \pm 1.1\ M^{-1}\ h^{-1}$ and $k_{-3} = (9.2 \pm 5.6) \times 10^{-4}\ h^{-1}$.

If Mg^{2+} binding is the rate-limiting step in the AP conformational conversion, it is possible that when the two metals are present, faster Zn^{2+} binding to the A and B sites acts to inhibit Mg^{2+} binding. To test this hypothesis, a stoichiometric amount of Zn^{2+} (4 mol per dimer) and an excess of Mg^{2+} were added to apo-AP in either order before assaying the protein's lability. Figure 7 shows the clear increase in the fraction of low-lability AP when the Mg^{2+} was added first, while the experiment where Zn^{2+} was added first produced nearly 100% high-lability AP. It thus appears that bound Zn^{2+} hinders Mg^{2+} binding, thereby keeping the AP in a more labile state.

It is established that while Zn^{2+} is responsible for the majority of the enzymatic activity of AP, Mg^{2+} binding acts to further increase this activity (*13*). As Mg^{2+} binds and converts AP from a high-lability to a low-lability species, one would expect a direct correlation between the increase in AP activity and in the fraction of AP in the low-lability

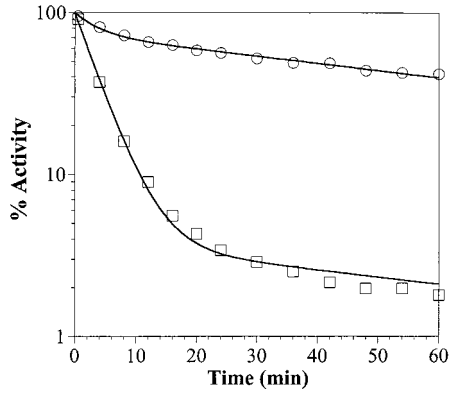

FIGURE 7: AP lability dependence on order of addition of metals. Lability curves for 0.5 mg/mL apo-AP with both 21 μM $ZnCl_2$ (4 equiv) and 0.1 mM $MgCl_2$ added: ○, $MgCl_2$ added first; □, $ZnCl_2$ added first. The fraction of high-lability AP was 0.73 and 0.04, respectively. The AP was incubated for 2 h with the first metal and then for 10 min after the addition of the second metal before the lability assay.

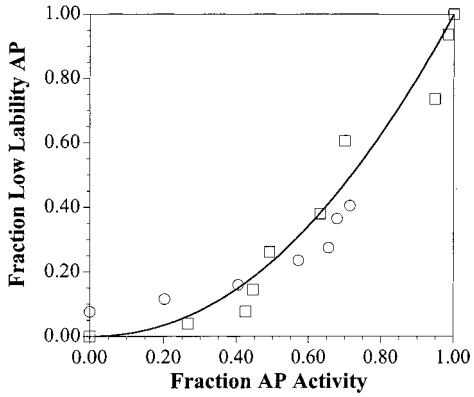

FIGURE 8: Correlation between fraction of increased activity and fraction of low-lability AP. (○) 0.1 mM $ZnCl_2$ and 0.1 mM $MgCl_2$ were added to 1.1 μM refolding AP, and activity and lability were measured over time. (□) 0.1 mM $ZnCl_2$ and various levels of $MgCl_2$ from 5 μM to 5 mM were added to 1.1 μM apo-AP, and activity and lability were measured after equilibrium was achieved. The fractional activity represented here reflects the relative activity increase over the Zn-AP activity. The solid line represents a best power-law fit of the equilibrium data, fraction lability = (fraction increase activity)$^{2.1}$, which agrees well with a binding model where the fraction of the low-lability state is equal to the square of the fractional increase in activity.

form. We have tested this correlation by measuring both lability and activity in a sample of refolding AP over time as Mg^{2+} binds, as well as in samples of AP that have been fully equilibrated with increasing concentrations of Mg^{2+}. The results of both kinetic and equilibrium approaches are shown in Figure 8. This plot correlates two variables, each dependent on Mg^{2+} binding, and reveals similar results for both experiments. Moreover, a clear nonlinear relationship between the increase in activity and the fraction of low-lability AP is revealed. The solid curve is a power-law fit to the equilibrium data, which yields an exponent of 2.1 ± 0.2, suggesting that the low-lability species most likely represents AP with two bound Mg^{2+}, while enzyme containing one Mg^{2+} per dimer is still in the high-lability state.

DISCUSSION

In the present study we investigated the molecular basis of the slow conversion of the AP species that is highly susceptible to GdnHCl denaturation (high-lability state) to the species with a slower rate of denaturation (low-lability state) that we have previously observed during in vitro renaturation of fully denatured AP (*9*, *26*). The lifetime of the conversion reaction between these species at 25 °C is 294 h, as shown in Figure 2. The current study tested the role played by metal binding in this slow conversion. To this end, we added Zn^{2+} and Mg^{2+} to a metal-free (apo) AP, a species that is known to maintain a folded and dimerized structure (*30*−*33*). The results of this experiment demonstrate that polypeptide-folding events, including subunit dimerization, are not the cause of the slow formation of the low-lability state. For example, 2 h after Zn^{2+} and Mg^{2+} addition to a completely folded apo-AP, the majority of the protein is still in the high-lability state (Figure 4). This is very similar to the behavior seen using holo-AP that has been completely denatured and refolded. Since both refolded AP and apo-AP with added metals denature with very similar kinetics, with decay times of 6.3 and 93.5 min for the refolded AP and 6.6 and 92.3 min for the apo-AP with added metals, we conclude that in both cases the same species of AP are present. Following a first-order reaction, with a lifetime of ca. 300 h, this high-lability AP converts to the low-lability state. This, again, is on a time scale similar to that seen in the conformational change of AP that has been denatured and refolded. Thus it appears that the addition of Zn^{2+} and Mg^{2+} to a folded apo-AP reproduces the two lability states, as well as the same long lifetime for conformational conversion as observed when AP is completely denatured and refolded in the presence of Zn^{2+} and Mg^{2+}.

In contrast, apo-AP to which only Zn^{2+} is added displays single exponential GdnHCl denaturation kinetics with a decay time of 4.7 min that does not change even after a long incubation time. This decay time is somewhat shorter than that of the high-lability component of AP when both metals are present. The complete absence of the slow, 92 min, decay species seen when both metals are present suggests that the low-lability species is associated with Mg^{2+} binding. The simplest explanation for these observations is that the species showing the 4.7 min decay represents Zn-AP, the 6 min decay species, if indeed a distinct AP form may in addition have one Mg^{2+} bound (or a combination of species with zero and one Mg^{2+} bound), and the species associated with the 92 min decay represents AP with two Mg^{2+} bound.

Both Zn^{2+} and Mg^{2+} are necessary for the production of fully stable and fully active AP (*11*, *12*). The binding of the four Zn^{2+} ions per dimer by far has the largest effect on AP, increasing the resistance to thermal denaturation (Figure 3B) and producing most of the thermodynamic stability and enzymatic activity (*13*, *34*−*36*). By contrast, the binding of two Mg^{2+} ions per dimer serves to slightly enhance these factors when added to Zn-AP but provides little stability and no activity when bound alone (*35*). These facts are consistent with our present observation that it is Mg^{2+} binding to Zn-AP that produces the low-lability AP. Just as Mg^{2+} increases the thermodynamic stability of Zn-AP, from $\Delta G = 120$ kcal/mol to $\Delta G = 130$ kcal/mol (*34*), it also increases the kinetic resistance of AP to denaturation, as seen in the much slower rate of unfolding. This greater denaturation resistance is related to the activation energy of unfolding, not thermodynamic stability, but it would be reasonable to expect that an increase in the latter stability would be accompanied by an

increased denaturation time. Mg^{2+} serves to increase both of these factors when added to Zn-AP, though the increase in denaturation time is much more dramatic.

The binding of Mg^{2+} to Zn-AP could lead to a low-lability protein in one of several ways, as shown in Figure 5. Mg^{2+} binding could lower the activation energy of a subsequent rate-limiting conformational change that produces the low-lability species (pathway 1). Alternatively, there could be a rate-limiting conversion of a Zn-AP species to a conformation that could then bind Mg^{2+} quickly to produce the low-lability state (pathway 2). Finally, Mg^{2+} binding itself could be the rate-limiting step that produces the low-lability species (pathway 3). The observed conversion of the high-lability to the low-lability state would in the case of pathway 3 provide evidence for slow Mg^{2+} binding, rather than rate-limiting conformational changes within AP. The results shown in Figure 6 resolve these possibilities, showing a linear dependence of the rate of lability state conversion on the concentration of Mg^{2+}. Only pathway 3 would be expected to show such a Mg^{2+} concentration dependence, since the other pathways are rate limited by internal conformational changes that are independent of the Mg^{2+} binding rate. The overall lability conversion rate (k_{obs}) for the reversible binding reaction shown for pathway 3 in Figure 5 can be resolved into its two constituent rate constants from the slope and intercept, yielding the forward rate $k_3 = 29.3 \pm 1.1\ M^{-1}\ h^{-1}$ and the reverse rate $k_{-3} = (9.2 \pm 5.6) \times 10^{-4}\ h^{-1}$.

The above experiments show that the slow conformational change in AP is due to slow Mg^{2+} binding to Zn-AP. One likely explanation for this slow rate is that bound Zn^{2+} impedes Mg^{2+} binding. Although Zn^{2+} bound to AP increases the association constant for Mg^{2+} (*13*), it may also serve to kinetically slow the binding process, either by physically occupying the Mg^{2+} site or by inhibiting Mg^{2+} entry. The results shown in Figure 7 support this view and clearly demonstrate that adding Zn^{2+} before Mg^{2+} dramatically hinders the Mg^{2+} binding, as reflected by the predominance of the high-lability enzyme. Conversely, adding Mg^{2+} first quickly produces mostly the low-lability species. Clearly, the Mg^{2+} rapidly binds in the absence of Zn^{2+}, and having pre-bound Zn^{2+} slows the binding of Mg^{2+}. This order-of-addition experiment also provides additional insight into the mechanism of Zn^{2+} blockage of Mg^{2+} binding. Since a stoichiometric amount of Zn^{2+} has been added to occupy the four Zn^{2+} binding sites per dimer, the Mg^{2+} sites remain free. We, therefore, conclude that the Zn^{2+} inhibition of Mg^{2+} binding cannot be caused by the direct occupation of Mg^{2+} binding sites, but rather by Zn^{2+} bound in its own A and B sites. An examination of the AP structure reveals that bound Zn^{2+} does not directly block access to the Mg^{2+} site but rather that there is a clear path from solution to the site (*11*). It thus appears that Zn^{2+} binding creates an AP conformation that dramatically slows the rate of Mg^{2+} binding in a more complicated manner. This result is in agreement with previous studies that have shown very slow exchange of $^{65}Zn^{2+}$ with unlabeled Zn^{2+} on the order of hundreds of hours, with even slower exchange times in the presence of bound Mg^{2+} and phosphate (*14*). The present study demonstrates that bound Zn^{2+} also causes slow Mg^{2+} binding. Increasing levels of Zn^{2+} will result in the direct occupation of the Mg^{2+} site (*13*), further inhibiting the conversion to the low-lability AP state, due to metal competition for that site.

Mg^{2+} is known to increase the enzymatic activity of Zn-AP (*13*), and since the Mg^{2+}-bound AP is also the low-lability species, there should exist a clear relationship between the fraction of low-lability AP and the activity of the enzyme. Figure 8 shows the correlation between the time-dependent increase in the fractional activity and the fraction of the low-lability AP, as Mg^{2+} binding approaches equilibrium. Also correlated are the increase in activity and the fraction of enzyme in low-lability state that are observed under equilibrium conditions established using increasing Mg^{2+} concentration (to push the equilibrium toward the Mg^{2+} bound state). In both kinetic and equilibrium experiments, the correlation is nonlinear. The solid curve in Figure 8 is a power-law fit of the equilibrium data, which yields an exponent of 2.1 ± 0.2. Thus the fraction of low-lability AP is related to the square of the fractional increase in activity due to Mg^{2+} binding. This is consistent with a Mg^{2+} binding model where the increase in activity depends linearly on total Mg^{2+} content of AP (each Mg^{2+} bound contributes equally to activity) but where two bound Mg^{2+} per dimer are needed to form the low-lability state. This result is also consistent with the linear dependence between Mg^{2+} concentration and lability conversion rate shown in Figure 6, as this rate likely reflects the binding of the second Mg^{2+} to AP. To support the hypothesis that two bound Mg^{2+} produce the low-lability state, it would be ideal to directly measure the concentrations of free and bound Mg^{2+} and to compare these data to the lability measurements. Preliminary attempts to conduct this experiment by detection of Mg^{2+} with fluorescent probes have not been successful, due to the interference of Zn^{2+} in the assays.

The effect of Mg^{2+} binding on the denaturation resistance of AP appears to be a nonlinear one. The lability decay kinetics and the activity/lability correlation suggest that the binding of one Mg^{2+} per AP dimer increases denaturation resistance slightly when compared to the Zn-AP but that two bound Mg^{2+} increase denaturation resistance much more significantly. Thus the overall structural impact of the second bound Mg^{2+} is much greater than that of the first. In general, this differential structural impact could be due to significant differences in subunit structure or to subunit interactions that occur upon ligand binding. The AP monomers are identical in sequence (*10*) and nearly identical in structure. The distances between the metal ligands are very similar in both monomers, with Zn_1-Zn_2 distances of 3.94 and 4.18 Å, Zn_1-Mg distances of 7.09 and 7.08 Å, and the Zn_2-Mg distances of 4.88 and 4.66 Å (*12*). The slight structural differences may contribute to the much greater impact that the second Mg^{2+} has upon the rate of GdnHCl inactivation. However, it appears more likely that Mg^{2+} binding causes long-range intersubunit interactions that change the overall AP structure significantly. This agrees with previous results from experiments with trypsin-modified AP hybrid dimers which revealed that the modified subunit altered the structural and kinetic properties of the other subunit through subunit interactions (*18*−*21*). NMR studies of metal hybrid AP dimers, with Zn^{2+} bound to one subunit and Cd^{2+} bound to the other, have found that Zn^{2+} binding caused substantial changes in the chemical shift of the Cd^{2+} ligands over 30 Å away at the other active site, again demonstrating long distance subunit interactions (*17*). Equilibrium metal binding studies have demonstrated that the binding of the second set

of Zn^{2+} ligands to the B sites greatly stabilizes both A and B site Zn^{2+} ligand pairs, which demonstrates the ability of metal binding to cause significant structural changes in AP (*14*). The present study demonstrates a similar role for Mg^{2+} binding. The long distance conformational changes that occur in AP upon Mg^{2+} binding are suggested by the results of a time-resolved crystallographic analysis of the D153G apo-AP mutant as metals are slowly reintroduced into the structure (*37*, *38*). This study revealed that, with metals absent, there is a disordered surface loop composed of residues 406−410 at the dimer interface, over 20 Å away from the Mg^{2+} binding sites. The movement of these residues can be triggered by Mg^{2+} binding at the active site through the shift in the position of the Mg^{2+} coordinating Asp51 and the subsequent shifting of a connecting helix. This provides a plausible mechanism for long distance structural change due to Mg^{2+} binding.

The experiments described in this work show that the previously observed slow transition from the high-lability AP state to the low-lability conformation is likely caused by slow binding of Mg^{2+} to Zn^{2+}-bound AP. The physiological consequences of this dramatic slowing of Mg^{2+} binding by Zn^{2+} are significant. In vivo, AP folds in the presence of both metals. Mg^{2+} concentrations in cells and serum have been measured in the range of 0.1−1.5 mM (*39*−*41*), which is the range used in the experiments presented here. Depending on the protein turnover rate, and the local concentration of Mg^{2+}, the majority of the AP molecules may exist for a significant fraction of their dwell time in the cell in the Zn-AP state, thus having lower stability and activity than the maximum possible. Well-established examples of slow events in protein maturation, such as proline isomerization and disulfide bond formation/shuffling, have been shown to be accelerated by the action of the enzyme catalysts peptidyl−prolyl isomerase and DsbA (*42*, *43*). In the present case of slow metal binding to a folded protein, an analogous solution would require assistance from a metal insertion catalyst to accelerate the binding process. Whether the actual in vivo metal binding by AP is dramatically different from the in vitro situation, due to cellular mechanisms that are absent in vitro, to high periplasmic concentrations of Mg^{2+}, or to the effect of high levels of tightly bound phosphate, requires further study.

This study also addresses the question of what purpose Mg^{2+} binding serves for AP, when most of the activity and stability are already provided by Zn^{2+} binding. The model proposed for Mg^{2+} binding and its relation to the formation of the low-lability state provides a possible answer. The binding of one Mg^{2+} per enzyme dimer appears to cause a slight slowing down of the GdnHCl denaturation reaction; however, two bound Mg^{2+} have a dramatic protection effect. Thus, just as Zn^{2+} provides AP with substantial thermodynamic stability, Mg^{2+} provides kinetic stability, slowing down the unfolding of AP under hostile, denaturing, conditions (e.g., low pH, high temperature, presence of proteases). This model also provides insight into why a dimeric structure is advantageous for AP. The significant increase in protection upon binding the second Mg^{2+} would be lost if AP were a monomer, as there would be no mechanism for structural adjustments via intersubunit communication. This may be a result that has general applicability to multimeric enzymes with metal ligands.

ACKNOWLEDGMENT

We thank Dr. E. R. Kantrowitz for the generous gift of the *E. coli* strain SM547 and the plasmid pEK154 and Kathleen Wisser for the AP expression and extraction work.

REFERENCES

1. Anfinsen, C. B. (1973) *Science 181*, 223−230.
2. Creighton, T. E. (1990) *Biochem. J. 270*, 1−16.
3. Jaenicke, R. (1999) *Prog. Biophys. Mol. Biol. 71*, 155−241.
4. Schmid, F. X. (1992) in *Protein Folding* (Creighton, T. E., Ed.) pp 197−241, W. H. Freeman and Co., New York.
5. Creighton, T. E. (1992) in *Protein Folding* (Creighton, T. E., Ed.) pp 301−351, W. H. Freeman and Co., New York.
6. Schiene, C., and Fischer, G. (2000) *Curr. Opin. Struct. Biol. 10*, 40−45.
7. Garel, J.-R. (1992) in *Protein Folding* (Creighton, T. E., Ed.) pp 405−454, W. H. Freeman and Co., New York.
8. Jaenicke, R. (1987) *Prog. Biophys. Mol. Biol. 49*, 117−237.
9. Subramanium, V., Bergenhem, N. C. H., Gafni, A., and Steel, D. G. (1995) *Biochemistry 34*, 1133−1136.
10. Bradshaw, R. A., Cancedda, F., Ericsson, L. H., Neumann, P. A., Piccoli, S. P., Schlesinger, M. J., Shriefer, K., and Walsh, K. A. (1981) *Proc. Natl. Acad. Sci. U.S.A. 78*, 3473−3477.
11. Kim, E. E., and Wyckoff, H. W. (1991) *J. Mol. Biol. 218*, 449−464.
12. Coleman, J. E. (1992) *Annu. Rev. Biophys. Biomol. Struct. 21*, 441−483.
13. Bosron, W. F., Anderson, R. A., Falk, M. C., Kennedy, F. S., and Vallee, B. L. (1977) *Biochemistry 16*, 610−614.
14. Coleman, J. E., Nakamura, K., and Chlebowski, J. F. (1983) *J. Biol. Chem. 258*, 386−395.
15. Gettins, P., and Coleman, J. E. (1983) *J. Biol. Chem. 258*, 396−407.
16. Gettins, P., and Coleman, J. E. (1983) *J. Biol. Chem. 258*, 408−416.
17. Gettins, P., and Coleman, J. E. (1984) *J. Biol. Chem. 259*, 4991−4997.
18. Roberts, C. H., and Chlebowski, J. F. (1984) *J. Biol. Chem. 259*, 729−733.
19. Roberts, C. H., and Chlebowski, J. F. (1985) *J. Biol. Chem. 260*, 7557−7561.
20. Tyler-Cross, R., Roberts, C. H., and Chlebowski, J. F. (1989) *J. Biol. Chem. 264*, 4523−4528.
21. Olafsdottir, S., and Chlebowski, J. F. (1989) *J. Biol. Chem. 264*, 4529−4535.
22. Brandts, J. F., Halvorson, H. R., and Brennan, M. (1975) *Biochemistry 14*, 4953−4963.
23. Cook, K. H., Schmid, F. X., and Baldwin, R. L. (1979) *Proc. Natl. Acad. Sci. U.S.A. 76*, 6157−6161.
24. Schmid, F. X. (1986) *Methods Enzymol. 131*, 70−82.
25. Keifhaber, T., Quaas, R., Hahn, U., and Schmid, F. X. (1990) *Biochemistry 29*, 3053−3061.
26. Dirnbach, E., Steel, D. G., and Gafni, A. (1999) *J. Biol. Chem. 274*, 4532−4536.
27. Chaidaroglou, A., Brezinski, D. J., Middleton, S. A., and Kantrowitz, E. R. (1988) *Biochemistry 27*, 8338−8343.
28. Malamy, M. H., and Horecker, B. L. (1964) *Biochemistry 3*, 1893−1897.
29. Garen, A., and Levinthal, C. (1960) *Biochim. Biophys. Acta 38*, 470−483.
30. Harris, M. I., and Coleman, J. E. (1968) *J. Biol. Chem. 243*, 5063−5073.
31. Applebury, M. L., and Coleman, J. E. (1969) *J. Biol. Chem. 244*, 308−318.
32. Reynolds, J. A., and Schlesinger, M. J. (1969) *Biochemistry 8*, 588−593.
33. Reynolds, J. A., and Schlesinger, M. J. (1967) *Biochemistry 6*, 3552−3559.
34. Chlebowski, J. F., and Mabrey, S. (1977) *J. Biol. Chem. 252*, 7042−7052.
35. Chlebowski, J. F., Mabrey, S., and Falk, M. C. (1979) *J. Biol. Chem. 254*, 5745−5753.

36. Trotman, C. N., and Greenwood, C. (1971) *Biochem J. 124*, 25−30.
37. Dealwis, C. G., Chen, L., Brennan, C., Mandecki, W., and Abad-Zapatero, C. (1995) *Protein Eng. 8*, 865−871.
38. Dealwis, C. G., Brennan, C., Christianson, K., Mandecki, W., and Abad-Zapatero, C. (1995) *Biochemistry 34*, 13967−13973.
39. Corkey, B. E., Duszynski, J., Rich, T. L., Matschinsky, B., and Williamson, J. R. (1986) *J. Biol. Chem. 261*, 2567−2574.
40. Heinonen, E., and Akerman, K. E. O. (1987) *Biochim. Biophys. Acta 898*, 331−337.
41. Ioannou, P. C., and Konstantianos, D. G. (1989) *Clin. Chem. 35*, 1492−1496.
42. Schonbrunner, E. R., Mayer, S., Tropschug, M., Fischer, G., Takahashi, N., and Schmid, F. X. (1991) *J. Biol. Chem. 266*, 3630−3635.
43. Bardwell, J. C. A., McGovern, K., and Beckwith, J. (1991) *Cell 67*, 581−589.

BI011399M